Raman Spectra of Phenylacetylene in Acetonitrile and Methylcyclohexane at Low Temperatures. 2. Structural Order and Vibrational Relaxation in Frozen Matrices at 77 K

H. Abramczyk,* G. Waliszewska, and M. Kołodziejski

Institute of Applied Radiation Chemistry, Technical University, 93-590 Lódź, Wróblewskiego 15, Poland

Received: April 16, 1998; In Final Form: July 21, 1998

Raman spectra of the ν_S(C≡C) stretching mode of phenylacetylene (PA) dissolved in acetonitrile and methylcyclohexane have been recorded at 77 K and compared with spectra in the liquid solutions at room temperature [Kołodziejski, M.; Waliszewska, G.; Abramczyk, H. *J. Phys. Chem. A* **1998**, *102*, 1918]. Substantial narrowing of spectra in frozen matrices at low temperatures leads to revealing of vibrational structure. The results given in this paper are a spectacular example of monitoring structural order going from liquid solutions to frozen matrices at low temperatures by Raman spectroscopy.

1. Introduction

Raman line shape and line width studies yield valuable insight into the structure around the molecular oscillator and the dynamics of vibrational energy states.[2−8] In going from isolated molecules in the gas phase through isotropic liquids to the solid-state phases of glasses and molecular crystals, we can monitor orientational order and changes in the dissipation of vibrational energy (energy relaxation) and loss of phase coherence (dephasing relaxation).

Study of Raman line shape can provide information on vibrational dynamics, mainly vibrational dephasing (T_2*), which may occur by a pure dephasing (T_2) and/or by energy relaxation (T_1). In pure dephasing relaxation, dynamic fluctuations of the oscillator frequency destroy the phase relationship. The dephasing caused by T_1 relaxation results from the change of the oscillator phase during the energy exchange which occurs in the process of the depopulation of vibrational states. Since both the frequency fluctuations and energy relaxation are due to intra- and intermolecular interactions of the oscillator with the surrounding molecules, the dephasing provides information about the dynamics of interactions and molecular motions around the oscillator. The Raman line shape study can yield meaningful information about the vibrational dynamics only if the vibrational band is homogeneously broadened by dephasing relaxation and not by inhomogeneous broadening. On the other hand, if the line width is dominated by inhomogeneous broadening, we can monitor structural disorder in the liquid phase, inhomogeneities in crystals, and glasses at low temperatures.

A considerable amount of experimental and theoretical information has been accumulated on the vibrational dynamics in liquids and molecular solids using conventional IR and Raman spectroscopy and nonlinear methods such as coherent antistokes Raman spectroscopy,[9] Raman echo,[3] and IR echo.[5] The time-resolved coherent Raman spectroscopy using single excitation pulse techniques provides information about the same dephasing time T_2 as conventional linear vibrational spectroscopy and, like it, suffers from the same inability to separate the various contributions to the observed line shape. Two or more excitation pulses techniques such as IR echo[5] or Raman echo[3] can extract the homogeneous vibrational line shape, even when the line shape is broadened significantly by inhomogeneous contributions.

The vibrational dynamics of liquids is fairly well-understood, and theoretical models and computer simulations dealing with the vibrational states in liquids and their interactions exist in the literature.[10−18] In liquids the fast vibrational dephasing accounts for the dominant part of the homogeneous line width at ambient temperature.[2] However, under certain circumstances, vibrational line shapes are dominated by inhomogeneous broadening.[3,5] The theoretical models for liquids use the concept of vibrations localized on molecules treated as the statistical ensamble and involving the ensamble-averaged density matrix of the individual molecules[2,10−15]

The theoretical models of vibrational dephasing in crystals use a quantum mechanical rather than a statistical framework in treating the collection of molecules in the sample and apply the Frenkel exciton formalism[19−23] in the interpretation of experimental data. The intramolecular vibrational states are considered to be extended crystal states due to the periodicity of the crystal state Hamiltonian rather than being localized on each molecule. Molecular crystals have traditionally fulfilled the role of model systems for understanding the dissipation of excess vibrational energy in the solid-state phase. In some molecular crystals such as naphthalene,[20] the T_2 processes at low temperatures are negligible and the homogoneous line broadening is dominated by T_1 processes.

Much less is known about vibrational relaxation in glasses. Vibrational relaxation in glass phases of low-temperature frozen matrices can be vastly different from those of its liquid and crystal counterparts. Not only the energy relaxation T_1 but also the phase relaxation T_2 can differ due to the effects of interactions of the solute with the solvent molecules and the different time scale of these processes. The dynamics of vibrational relaxation T_1 and T_2 proceed on a much slower time scale, and the relation $T_1 > T_2$ valid in liquids may not be fulfilled. Additionaly, it can be expected that the rigid environment of the solute leads to significant inhomogeneous band broadening in glasses. Although a general outline of the dynamics in glasses has been developed,[24,25] the fundamental issues of vibrational dynamics remain to be clarified. There is a limited number of papers on vibrational relaxation in glasses. The recent results[5] which are the first ones on the temperature

S1089-5639(98)01884-2 CCC: $15.00
Published on Web 09/11/1998

dependence of vibrational dephasing in organic glasses show that at low temperatures below the glass transition temperature the energy relaxation T_1 is the dominant contribution to the homogeneous line width and the contributions from pure dephasing are negligible. Above 50 K pure dephasing T_2 and orientational relaxation make the major contributions to the IR line width, while above 150 K pure dephasing overwhelms the other contributions to the homogeneous line width. The comparison of the IR echo and IR absorption results shows that, at low temperatures below 150 K, the vibrational line of studied glasses is dominated by inhomogeneous broadening and the homogeneous contribution is negligible in the total bandwidth. Above 150 K the homogeneous line width begins to approach the measured absorption line width, and at 200 K the homogeneous and inhomogeneous contributions to the absorption line are of equal magnitude.

In this paper we present Raman spectra for phenylacetylene in acetonitrile and methylcyclohexane in frozen matrices at 77 K as a function of concentration and compare them with the spectra of their liquid counterparts. The results show spectacular changes and illustrate that Raman spectroscopy is very useful for monitoring structural order in going from isotropic liquids to solid-state phases at low temperatures.

Some phenylacetylenes are typical liquid crystal materials and are of particular interest with regard to the most recent liquid crystal technology which uses fluorinated diphenylacetylene (DPA) to achieve high-purity nematic materials.[26]

Nematic materials possess long-range orientational order but little if any positional order. This results in their properties being between those of isotropic liquids and crystalline solids. The molecules in these intermediate (meso-) phases behave like liquids in that they flow, but also they exhibit anisotropic properties of crystals such as birefrigence, optical anisotropy and long-range molecular order. The manifestation of this property at the molecular level is that, for typical nematogens, which tend to be approximately prolate spheroids, the long molecular axes tend to align in a preferred direction. The reorganization process from isotropic to the three-dimensional crystal lattice on cooling can be monitored with various spectroscopic techniques. Because of the optical anisotropy of liquid crystals, polarized absorption spectroscopy and Raman spectroscopy[6] are the techniques of choice for observing and investigating order-related phenomena. These techniques are very sensitive to changes in intermolecular structure that accompany transitions from the isotropic liquid phase through liquid crystalline phases with increasingly higher positional order to the crystalline solid. These structural changes are reflected in frequency shifts and sometimes drastic changes in intensities and line widths of the vibrational bands, leading to the disappearance of some bands and the appearance of new ones.

A great deal of work is still needed to establish the connections between vibrational spectra on one hand and molecular properties and intermolecular interactions in liquids, liquid crystals, glasses, and crystals on the other. One of the goals of the proposed work is to develop such connections through systematic spectroscopic studies and theoretical modeling. Since several aspects of the Raman and IR spectra of diphenylacetylene in solutions and solid matrices obtained by Abramczyk and co-workers[27] are not well-understood, we have studied the Raman and IR spectra of phenylacetylene in solutions and solid matrices. The results demonstrate drastic changes occur in the C≡C stretch Raman bands of PA as a function of temperature. The bands also exhibit a strong solvent dependence.

CHART 1

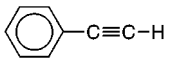

phenylacetylene (PA)

The goal of the proposed research is to uncover the molecular basis for the observed behavior and to obtain a more complete picture of the structure and dynamics of PA in different condensed-phase environments. Vibrational spectroscopy will also be used to determine if these molecules exhibit liquid crystalline phases and, if they do, to characterize them. As far as we know the Raman spectra of phenylacetylene at low temperatures have never been reported before.

2. Experiment

Spectrograde acetonitrile, methylcyclohexane, and phenylacetylene (Chart 1) were purchased from Aldrich. Acetonitrile and methylcyclohexane was used without further purification. Phenylacetylene was distillated under vacuum before solutions were prepared. The solutions of PA in acetonitrile and methylcyclohexane were made with concentrations varied for the phenylacetylene mole fraction x_{PA} from $x_{PA} = 0.0$ to $x_{PA} = 1.0$. Raman spectra were measured with a Ramanor U1000 (Jobin Yvon) and a Spectra Physics 2017S argon ion laser operating at 514 nm. The C≡C stretching mode of PA in acetonitrile and methylcyclohexane were measured. Spectra were recorded at room temperature and at 77 K in a nitrogen bath cryostat. The spectral slit width was 1.3 cm^{-1}, both at room temperature and at 77 K. The signal-to-noise ratio in liquid solutions is about 100:1. A similar ratio is observed in frozen matrices at higher concentrations of PA, whereas at lower concentrations the ratio is lower, being about 20:1 in the worst cases. The smaller ratios come from the fact that measurements in the cryostat always give lower intensities of the signals, and the presence of liquid nitrogen results in small fluctuations of the scattered light intensities. A polarization analyzer and $\lambda/4$ waveplate were used to select polarized (VV) and depolarized (VH) components. The isotropic Raman spectra were calculated according to the relation

$$I_{iso} = I_{VV} - {}^4/_3 I_{VH} \tag{1}$$

The depolarization ratio defined as

$$\rho = I_{VH}/I_{VV} \tag{2}$$

was measured for each sample.

The interference filter has been used to purify the laser line by removing additional natural emission lines which interfere with the Raman lines, especially in the case of solid samples.

We have taken into account the instrumental bandbroadening (1.3 cm^{-1}), which coresponds to the 200 μm mechanical slit of the spectrometer. We have calculated the experimental bandwidths after the deconvolution procedure was corrected for finite slit width according to the formula[28]

$$\Delta^t_{1/2} = \Delta^a_{1/2}(1 - 2(s/\Delta^a_{1/2})^2)^{1/2} \tag{3}$$

where the superscripts t and a denote "true" and "apparent" and s is the spectral slit width.

3. Results

In this section we present the Raman spectra of phenylacetylene in acetonitrile and methylacetylene in liquid solutions at

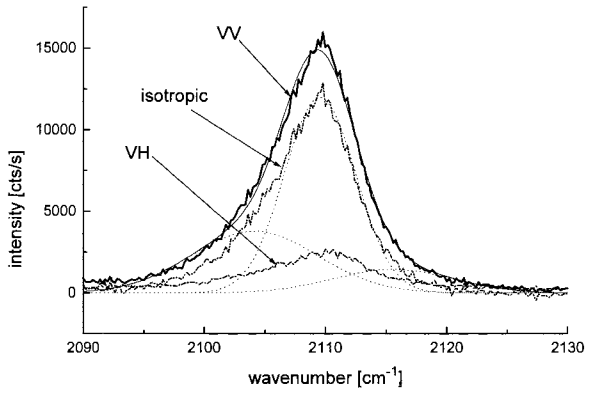

Figure 1. VV, VH, and isotropic Raman spectra of the C≡C stretching mode of phenylacetylene in acetonitrile (c = 4.01 mol/dm^3) at room temperature: --, VV component after deconvolution into three Gaussians.

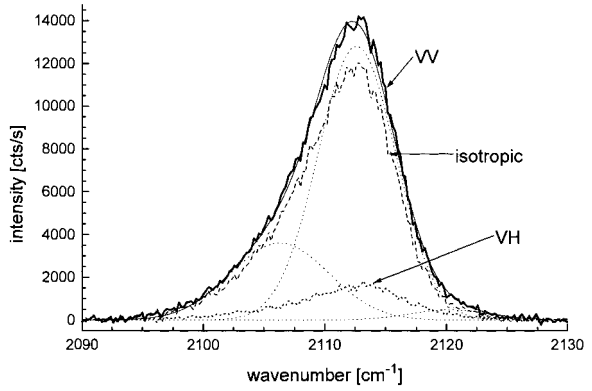

Figure 2. VV, VH, and isotropic Raman spectra of the C≡C stretching mode of phenylacetylene in methylcyclohexane (c = 5.37 mol/dm^3) at room temperature: -- VV component after deconvolution into three Gaussians.

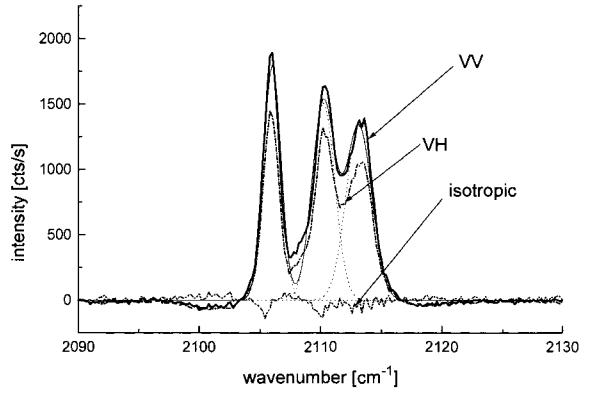

Figure 3. VV, VH, and isotropic Raman spectra of the C≡C stretching mode of phenylacetylene in acetonitrile (c = 4.51 mol/dm^3) at 77 K: --, VV component after deconvolution into three Gaussians.

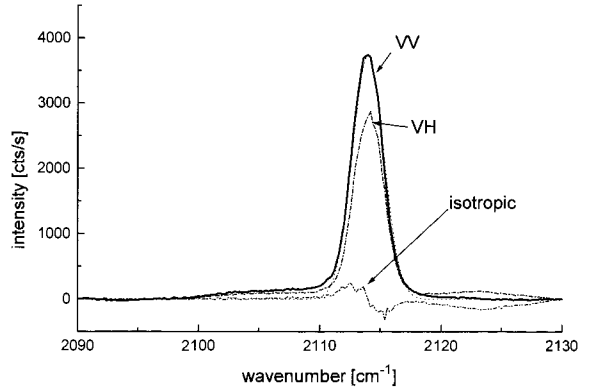

Figure 4. VV, VH, and isotropic Raman spectra of the C≡C stretching mode of phenylacetylene in methylcyclohexane (4.48 mol/dm^3) at 77 K.

room temperatures and in solid-state frozen matrices at low temperature (77 K).

Figure 1 shows the VV, VH, and isotropic Raman spectra of the C≡C stretching mode ν_s(C≡C) of PA in acetonitrile at c = 4.01 mol/dm^3 at room temperature. The bands are broad and slightly asymmetric on the low-frequency side. The depolarization ratio is $\rho = 0.16$.

In Figure 2 the VV, VH, and isotropic Raman spectra of the C≡C stretching mode ν_s(C≡C) of PA in methylcyclohexane at c = 5.37 mol/dm^3 at room temperature are shown. Also in this case the bands are slightly asymmetric on the low-frequency side. The depolarization ratio is $\rho = 0.11$

In Figure 3 the VV, VH, and isotropic Raman spectra of the C≡C stretching mode ν_s(C≡C) of PA in acetonitrile at c = 4.51 mol/dm^3 in solid frozen matrix at 77 K are shown. The comparison of the Raman spectra at 77 K to that in liquid solution at room temperature in Figure 1 shows that the broad band observed in liquid solution is split into three narrow components with peaks at 2106.0, 2110.2, and 2113.2 cm^{-1}. The three components with Gaussian contours have the bandwidths 1.43, 1.88, and 2.10 cm^{-1}, respectively. The depolarization ratio is $\rho = 0.75$.

In Figure 4 the VV, VH, and isotropic Raman spectra of the C≡C stretching mode ν_s(C≡C) of PA in methylcyclohexane at concentration c = 4.48 mol/dm^3 in solid frozen matrix at 77 K are shown. Although the concentration of PA in methylcyclohexane is nearly the same as that for PA in acetonitrile in Figure 3, the spectra differ significantly. Instead of the three peaks observed in acetonitrile we observe only one narrow peak at 2114.0 cm^{-1} with the bandwidth of 2.56 cm^{-1}. The bandwidth of PA in methylcyclohexane is a little greater than that observed in acetonitrile. The depolarization ratio is 0.75.

The comparison between the bandwidths observed in liquid solutions and solid matrices shows substantial narrowing at low temperatures. The marked difference between intensities of isotropic components in the liquid solution and in the frozen matrix is observed. Indeed, the intensities of the isotropic components decrease drastically both in acetonitrile and methylcyclohexane matrices in comparison with their liquid counterparts, and the depolarization ratios increase markedly from 0.16 in liquid acetonitrile and 0.11 in methylcyclohexane to 0.60−0.75 in frozen matrices at comparable concentrations.

To explain the differences between the spectra of PA in acetonitrile and in methylcyclohexane, we examined how the band shape and the bandwidths depend on concentration.

In Figure 5 we show the VV Raman components at 77 K for the ν_s(C≡C) mode of PA in methylcyclohexane at three concentrations: c = 0.334, 0.91, 4.48 mol/dm^3 with the intensities normalized to the intensity at c = 4.48 mol/dm^3. We can see that at lower concentrations of PA in methylcyclohexane the structureless bands are broad with bandwidths similar to those observed in liquid solutions. The experimental bandwidth for c = 0.334 mol/dm^3 is 9.76 cm^{-1}. When fitted with two Gaussians with the peaks at 2105.7 and 2112.2 cm^{-1}, the bandwidths are 5.65 and 7.72 cm^{-1}. At c = 0.91 mol/dm^3 the band is also broad with the peaks at nearly the same frequencies and the bandwidths 7.12 and 3.88 cm^{-1}, respectively. So, the significant band narrowing is observed for the higher frequency component. At the concentrations from about c = 1.58 to 4.48

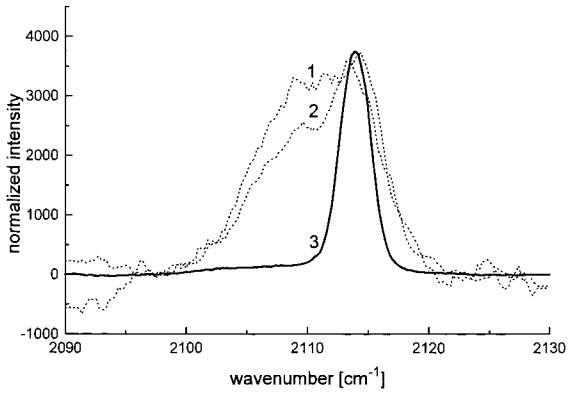

Figure 5. VV Raman spectra of the C≡C stretching mode of phenylacetylene in methylcyclohexane at 77 K: 1, $c = 0.334$ mol/dm^3; 2, $c = 0.91$ mol/dm^3; 3, $c = 4.48$ mol/dm^3.

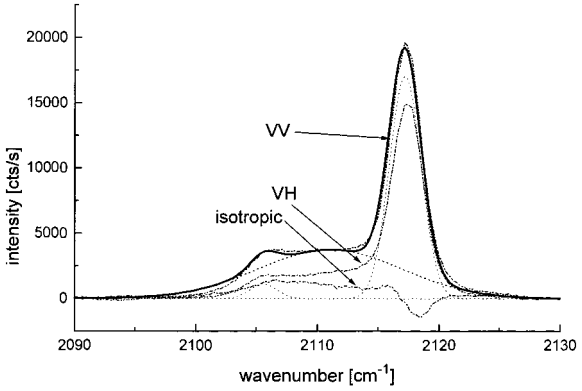

Figure 6. VV, VH, and isotropic Raman spectra of the C≡C stretching mode of phenylacetylene in methylcyclohexane (6.48 mol/dm^3) at 77 K: --, VV component after deconvolution into three Gaussians.

mol/dm^3, the intensity of the low-frequency component decreases and we observe only one narrow peak at about 2114.0 cm^{-1} with the bandwidth decreasing with the increase of PA concentration.

In Figure 6 the VV, VH, and isotropic Raman spectra of the C≡C stretching mode ν_s(C≡C) of PA in methylcyclohexane at concentration $c = 6.48$ mol/dm^3 in solid frozen matrix at 77 K are shown. Although the main peak at 2117.5 cm^{-1} has a shape and bandwidth similar to those for PA at the concentration of $c = 4.48$ mol/dm^3, we can observe that the new, broad, flat band appears on the low-frequency side. This new, structureless band becomes to split at higher PA concentrations, which is clearly shown in Figure 7.

The VV, VH, and isotropic Raman spectra of neat PA are shown in Figure 7. As we can see, the best fit to the experimental data are obtained with four Gaussians with the peaks at 2106.1, 2111.7, 2114.9, and 2117.2 cm^{-1} with the bandwidths 2.32, 1.93, 2.44, and 1.43 cm^{-1}, respectively.

In Figure 8 we have compared the concentration dependences of the Raman bandwidths (Figure 8a) and the maximum peak positions (Figure 8b) for VV components of the ν_s(C≡C) mode of PA in methylcyclohexane in liquid solutions and frozen matrices at 77 K. From Figure 8a we can see that, in contrast to liquid solutions, in frozen matrices at 77 K we observe the exponential decay of the PA bandwidth with increasing PA mole fraction. From Figure 8b we can see that also the concentration dependences for the maximum peak position have the opposite trends in liquid solution and in the frozen matrix.

The changes we observe in the Raman spectra of PA in methylcyclohexane seem to reflect first of all the structural

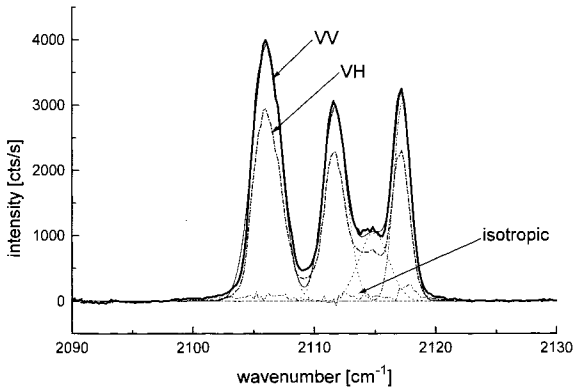

Figure 7. VV, VH and isotropic Raman spectra of the C≡C stretching mode of pure phenylacetylene at 77 K: --, VV component after deconvolution into four Gaussians.

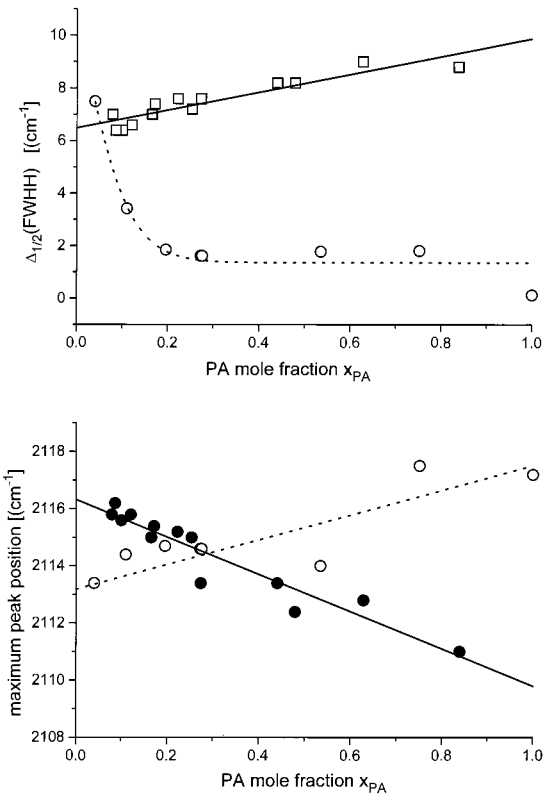

Figure 8. (a, top) Raman VV bandwidth $\Delta_{1/2}$(fwhh) of the C≡C stretching mode of phenylacetylene in methylcyclohexane as a function of phenylacetylene mole fraction x_{PA}: □, experimental data[1] at room temperature; ○, experimental data at 77 K; —, fitting of experimental data at room temperature ($\Delta_{1/2}$(fwhh)/cm^{-1} = 6.48 + 3.37x_{PA}); ···, fitting of experimental data at 77 K. (b, bottom) Raman VV maximum peak position of the C≡C stretching mode of phenylacetylene in methylcyclohexane as a function of phenylacetylene mole fraction x_{PA}: ●, experimental data[1] at room temperature; ○, experimental data at 77 K; —, fitting of experimenal data at room temperature (ν_0/cm^{-1} = 2116.32 − 6.53x_{PA}); ···, fitting of experimental data at 77 K (ν_0/cm^{-1} = 2113.18 + 4.31x_{PA}).

changes and increasing order in frozen matrices when the PA concentration increases. At a low concentration of PA, methylcyclohexane as the host matrix determines the structural properties. Methylcyclohexane is known to form glassy matrices. The structural disorder of a glassy matrix seems to lead to inhomogeneous broadening which is illustrated in Figures 5 and 8a. At higher concentrations of PA the structural properties of the matrix begin to depend on PA itself. The increasing order

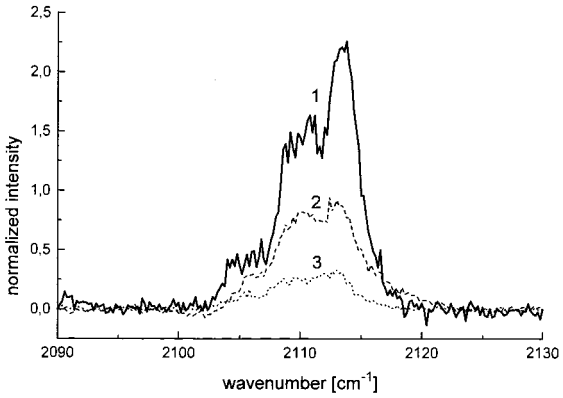

Figure 9. VV Raman spectra of the C≡C stretching mode of phenylacetylene in acetonitrile at 77 K: 1, $c = 0.334$ mol/dm^3; 2, $c = 0.91$ mol/dm^3; 3, $c = 2.21$ mol/dm^3.

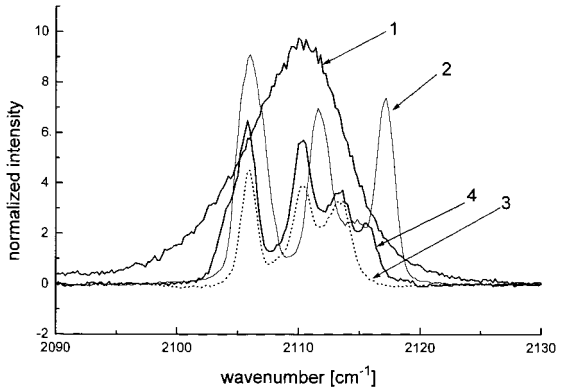

Figure 10. VV Raman spectra of the C≡C stretching mode of phenylacetylene in acetonitrile at 77 K: 1, neat PA in liquid state at room temperature; 2, neat PA at 77 K; 3, $c = 4.51$ mol/dm^3; 4, $c = 6.48$ mol/dm^3.

seems to lead to signifficant band narrowing of the ν_s(C≡C) mode of PA.

To learn more about the reason for the increasing order and the mechanisms of band narrowing, we have chosen for comparison acetonitrile in order to study the concentration dependence of the VV, VH, and isotropic Raman spectra in a polar environment, which forms a polycrystalline matrix at 77 K.

In Figure 9 we show the VV Raman components for the ν_s-(C≡C) mode of PA in acetonitrile at three concentrations $c = 0.334$, 0.91, and 2.21 mol/dm^3. Each component was normalized to unity and multiplied by the magnitude of the PA concentration.

In Figure 10 we show the VV Raman components for the ν_s(C≡C) mode of PA in acetonitrile at $c = 4.51$ and 6.48 mol/dm^3 and for comparison in neat PA at 77 K and at room temperature.

From Figures 9 and 10 we can see that at lower concentrations of PA in acetonitrile the bands are broad with bandwidths similar to those observed in the liquid solutions presented in Figure 1. At the concentration of PA of about $c = 1.58$ mol/dm^3 in acetonitrile, we notice that the structureless, broad band begins to split into three bands. This structure becomes more and more clear with the PA concentration increasing, and at $c = 4.51$ mol/dm^3, we observe a well-resolved three peak structure, with the peaks at 2106.0, 2110.2, and 2113.2 cm^{-1}. As the PA concentration reaches $c = 6.48$ mol/dm^3, we observe the building up of the additional peak at 2115.4 cm^{-1} in comparison with the structure seen for $c = 4.51$ mol/dm^3 (Figure 10). When

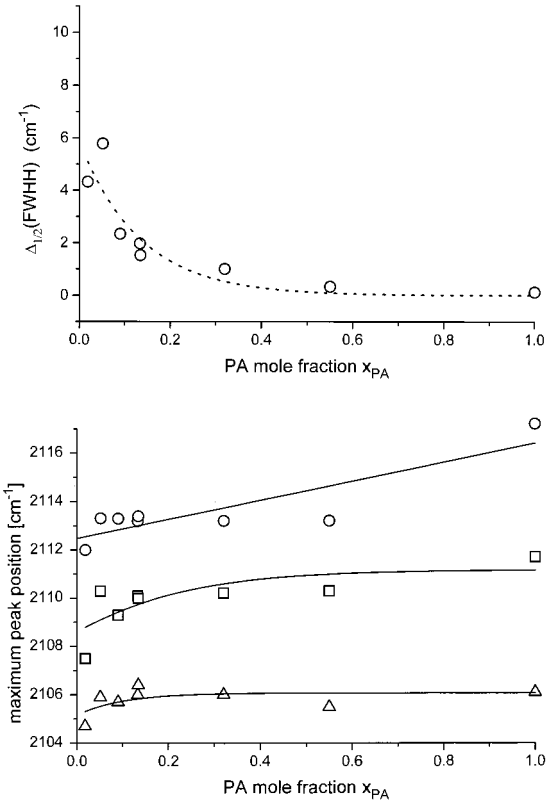

Figure 11. (a, top) Raman VV bandwidth $\Delta_{1/2}$(fwhh) of the C≡C stretching mode of phenylacetylene in acetonitrile for the peak at the highest frequency as a function of phenylacetylene mole fraction x_{PA}: ○, experimental data at 77 K; ···, fitting of experimental data at 77 K $\Delta_{1/2}$(fwhh)/cm^{-1} = 5.83 exp(−x_{PA}/0.133). (b, bottom) Raman VV maximum peak positions of the C≡C stretching mode of phenylacetylene in acetonitrile as a function of phenylacetylene mole fraction x_{PA}: ○, □, △, experimental data at 77 K for the band deconvoluted into three Gaussians.

the PA concentration increases, the peak at 2113.2 cm^{-1} dissappears while the intensity of the peak at 2115.4.cm^{-1} increases, shifting to 2117.2 cm^{-1} in neat PA at 77 K.

In Figure 11 we have shown the concentration dependences of the Raman bandwidths (Figure 11a) and the maximum peak positions (Figure 11b) for the VV components of the ν_s(C≡C) mode of PA in acetonitrile in frozen matrices at 77 K. We can see that, again in contrast to liquid solutions, in frozen matrices at 77 K we observe the decay of the PA bandwidth with an increasing PA mole fraction.

4. Discussion

The results illustrate that Raman band shape analysis provides an excellent method for monitoring structural order going from indicating random orientation isotropic liquids through partially ordered phases to increasing alignment in solid-state phases. In our previous paper[1] we have shown that for PA in methylcyclohexane in liquid solutions at room temperature the bandwidth of the ν_s(C≡C) mode increases linearly with increasing phenylacetylene mole fraction. The experimental concentration dependence has been reproduced very well by the theoretical model of vibrational dephasing, assuming that the hard repulsive collisions give the main contribution to the band broadening.[1]

From the comparison in Figure 8a between the bandwidths in liquid methylcyclohexane and the frozen matrix at the PA mole fraction close to zero, we can see that the bandwidth in glassy matrix is only about 1 cm^{-1} greater than in solution. At first it seems to suggest that at infinite dilution of PA, when

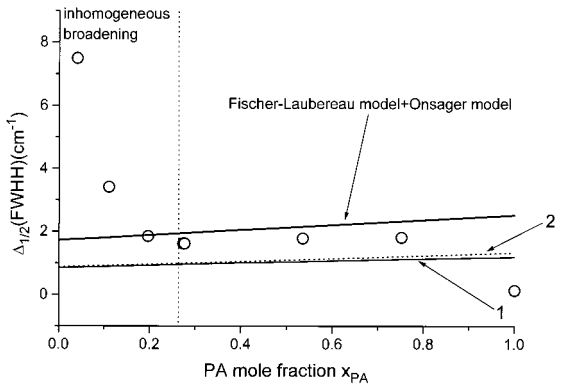

Figure 12. Raman VV bandwidth $\Delta_{1/2}$(fwhh) of the C≡C stretching mode of phenylacetylene in methylcyclohexane as a function of phenylacetylene mole fraction x_{PA}: ○, experimental data at 77 K; 1, Fischer−Laubereau theoretical model; 2, Onsager model; −, the sum from the both theoretical models.

the mechanism of structural alignment does not operate, the main contribution to the band broadening gives the hard collision homogeneous vibrational dephasing as in liquid solution at the same concentration. This conclusion is not true as we should remember that all the theories of vibrational dephasing,[2,10,12−15] except the hydrodynamic model of Oxtoby,[11] predict a decrease in the homogeneous line width with decreasing temperature. The isolated binary collision models of Fischer−Laubereau[12] and Schweizer−Chandler[13] predict a temperature dependence of $\Delta_{1/2}(\text{fwhh}) \propto \rho T^{3/2}\rho(\sigma)$, where fwhh is the full width at half-height. Assuming a mild temperature dependence for the radial distribution function $\rho(\sigma)$, we obtain that the bandwidth due to the hard collision homogeneous broadening at 77 K should decrease as much as $(77/298)^{3/2} = 0.13$ times in comparison with the widths at room temperature, giving only $7.72 \times 0.13 = 1.00$ cm^{-1}.

In Figure 12 we have shown the experimental bandwidths of the VV components of the ν_s(C≡C) mode of PA in methylcyclohexane compared with the theoretical bandwidths for $T =$ 77 K calculated from the Fischer−Laubereau model in the same way as in our previous paper for $T = 298$ K.[1] Besides the hard collision model of vibrational dephasing, we have tested the electrostatic models of vibrational dephasing such as the Onsager model and TD−D, TD−TD models described in detail in our previous paper.[1] We have found that the TD−D and TD−TD models give negligible contributions to the band broadening but the Onsager model gives a contribution of an order similar to that predicted from the Fischer−Laubereau model. The theoretical results obtained from the Onsager model are given in Figure 12. Unfortunately, the concentration dependences which are predicted from both the Fischer−Laubereau and Onsager models are very similar, and one cannot distinguish between them. None of the models separately reproduces satisfactorily the experimental data. However, it should be noticed that each of the models gives about half of the experimental bandwidth observed for PA concentration greater than about $x = 0.2$ and the sum of the contributions from both models reproduces quite well the concentration dependence between $x = 0.2$ and 0.7−0.8. It may suggest that in frozen matrices at PA concentrations greater than $x = 0.2$ both hard collisions and electrostatic interactions leading to pure vibrational dephasing T_2 are responsible for the band broadening. In this regard, the mechanism of vibrational dephasing in PA frozen matrices differs from that for liquid solutions of PA in methylcyclohexane at room temperature, where the band broadening in the whole range of concentrations was evidently dominated by homogeneous dephasing due to hard, repulsive collisions without the electrostatic contribution from the Onsager field. From the results presented here we can state that in frozen matrices at PA concentrations greater than $x = 0.2$ the hard collision dephasing still exists but it produces a much smaller effect on the band broadening than in the liquid phase and its contribution is comparable to that from dephasing due to electrostatic interations.

In contrast, it is evident from the results given in Figure 12 that for PA concentrations lower than $x = 0.2$ the homogeneous broadening due to collisions and/or electrostatic interactions cannot be applied and a quite different mechanism of broadening operates. At low concentrations of PA in methylcyclohexane the band broadening seems to come from vibrational dephasing occurring due to static or slowly relaxing disorder, giving rise to inhomogeneous broadening in the vibrational line shape. The amount of static disorder can be strongly dependent on the thermodynamic state of the sample and is expected to increase on going from the liquid to the glassy state. In our case it can be estimated as the difference between the experimental bandwidth and the theoretical bandwidth, being the sum of the Fischer−Laubereau and Onsager bandwidths. For the PA mole fraction close to zero it is equal to $7.72 - (1.0 + 0.9) = 5.82$ cm^{-1} and gives the dominant contribution to the band broadening.

The second important finding of this paper is the splitting of the band for the ν_s(C≡C) mode of PA in acetonitrile but not in methylcyclohexane. The splitting into a three peak structure begins to reveal at PA concentrations of about 1.5 mol/dm^3 ($x = 0.2$) and becomes more and more clear with the increasing of the PA concentration. The question arises, what is the origin of this effect? To answer this question, we should know more about the thermodynamic state of the frozen matrices. It would be very helpful to have an access to the crystallographic and thermodynamic data as a function of concentration for these systems which are not available in the literature at present. However, our results show evidently the increasing order with increasing PA concentration, and at concentrations greater than $x = 0.2$ the crystalline phase seems to dominate.

The vibrational spectra of molecular crystals is complicated by (a) Davydov splitting, (b) crystal-field splitting of degenerate modes, (c) combination bands, often intensified due to crystal state induced Fermi resonance, and (d) the presence of lattice phonons. The multiplet in the crystal spectrum can arise because of any of the above effects. At the moment we can exclude only the second reason for splitting. To determine the mechanism leading to the band splitting, we are studying the band shape in isotopic mixtures as a function of composition. The results will be published in a subsequent paper. The effectiveness of isotopic mixed crystal studies for determining the nature of the splitting is very important because the multiplet structure of the neat crystal is perurbed severly in the isotopic mixed crystal only for the first case, i.e., Davydov splitting.

Whatever the origin of the splitting is, it must come from the increasing contribution from the crystalline phase. However, it is interesting to notice that also in liquid acetonitrile solution (Figure 1) the band seems to consist of three peaks, although the structure cannot be seen because of the significant band broadening at room temperature. When the temperatures goes down, the three components become narrower, revealing the splitting into three peaks separated by about 5 cm^{-1}. It may suggest that the structural order in liquid solutions and frozen matrices at 77 K is in fact very similar. It is known that in crystals each vibration is split into MZ-fold states, where M is the number of unit cells and Z is the number of molecules in the unit cell. The interaction between Z molecules within the unit cell creates Z components. The broadening of each

component comes from the interactions between *M* translationally equivalent molecules forming the vibron band with components separated typically $10^{-2}-10^{-3}$ cm^{-1}. It seems that the three components observed in both liquid solutions and frozen matrices of PA in acetonitrile and methylcyclohexane result from the interactions between *Z* molecules within the unit cell. It would mean that $Z = 3$ (or 4 at some concentrations) in acetonitrile and $Z = 1$ in methylcyclohexane. Despite the splitting typical for crystalline solids, our results on mechanisms of band broadening for each component as a function of concentration disscussed above seem to suggest mechanisms typical for liquids rather than crystals with negligible contribution from vibron broadening due to the periodicity of the intermolecular potential.

5. Conclusions

The main focus of the proposed experimental studies was to learn more about the intermolecular structure and dynamics of PA in different condensed-phase environments. The environments that were considered include solutions of these molecules in polar and nonpolar solvents. Solute concentrations were varied in order to assess the role of solute−solute interactions and, at higher solute concentrations, to determine if and under what conditions nematic ordering occurs. The temperature effect on vibrational spectra was determined and analyzed.

The results presented here include three important findings: (1) the depolarization ratios ($\rho = I_{VH}/I_{VV}$) are temperature-dependent, (2) substantial narrowing of the C≡C band with decreasing temperature is observed both in acetonitrile and methylcyclohexane, contrary to expectations that inhomogeneous broadening should give a significant contribution at low temperatures, and (3) splitting of the band of the PA ν_s(C≡C) mode into three bands in acetonitrile matrices is observed but only one band is observed in methylcyclohexane.

Our results show a marked increase in the depolarization ratios in going from liquid solution to frozen (acetonitrile) and glassy (methylcyclohexane) solvents. This increase in ρ may be taken as evidence of increased ordering of PA in frozen matrices, composed of either polar or nonpolar solvents. At 77 K, the depolarization ratios of PA in acetonitrile are about 0.6−0.75, being as much as three times as large as those in liquid acetonitrile and methylcyclohexane. The depolarization ratios of PA in acetonitrile are a little larger than those for PA in methylcyclohexane at the same concentrations. This may suggests a higher degree of alignment in a polar, polycrystalline matrix (acetonitrile) than in a nonpolar, glassy one (methylcyclohexane). At this stage it is unclear what the structure of PA in frozen acetonitrile and methylcyclohexane is and to what extent the observed spectra are a manifestation of solute−solute interactions typical for nematic materials and the resulting structuring. However, our results show evidently that PA in solutions and pure PA have properties being between those of isotropic liquids and crystalline solids. We have shown that the mechanisms of vibrational dephasing in liquid and solid PA solutions are similar and typical for isotropic liquids. We have found the increasing contribution from long-range electrostatic interactions (Onsager model) with the temperature decreasing. On the other side, we have found the splitting of the PA ν_s-(C≡C) band and the change of the depolarization ratio with temperature and concentration, indicating anisotropic properties typical for crystals. We have found and estimated the contribution coming from inhomogeneous band broadening. The inhomogeneous broadening was found to be the dominant mechanism of vibrational dephasing for concentrations of PA from infinite dilution up to $c = 1.5$ mol/dm^3 both in acetonitrile and methylcyclohexane.

Further studies are needed to determine which types of solute−solute and solute−solvent intermolecular forces are chiefly responsible. Computer modeling and simulation as well as crystallographic studies would be very helpful in answering these questions as would experiments which probe the concentration dependence of the low-temperature spectra. A great deal of work is still needed to establish the connections between vibrational spectra on one hand and molecular properties and intermolecular interactions in liquid crystals on the other. One of the goals of the present paper was to start developing such connections through systematic spectroscopic studies.

Given that dramatic solvent effects on Raman bands at low temperature have been found, further studies will be carried out to determine which aspects of solute−solvent interactions are mainly responsible for these effects. Thus, in addition to acetonitrile, solutions of PA in other, structurally different, polar solvents, namely, alcohols, will be studied. The effects of solvent structure will also be studied in nonpolar solvents by investigating the spectra in cyclohexane, which is closer to being spherically symmetric than methylcyclohexane.

To explain the observed changes in depolarization ratios with temperature and solvent as well as the dependence of ρ on solute concentration, theoretical models for the reorientational correlation functions would be very helpful.

Acknowledgment. The authors gratefully acknowledge the support of this work by Programm Fastkin'97 of the Foundation for Polish Science. Support from KBN through grants 020/*T*09/97/12 and 3 T09 A 181 09 and Dz.S. 559/98 is also acknowledged.

References and Notes

(1) Kołodziejski, M.; Waliszewska, G.; Abramczyk, H. *J. Phys. Chem.* **1998**, *102*, 1918.
(2) Rotschild, W. G. *Dynamics of Molecular Liquids*; Wiley: New York, 1984.
(3) Muller, L. J.; Vanden Bout, D.; Berg, M. *J. Chem. Phys.* **1993**, *99*, 810.
(4) Trout, T. J.; Velsko, S.; Bozio, R.; Decola, P. L.; Hochstrasser, R. M. *J. Chem. Phys*. **1984**, *81*, 4746.
(5) Tokmakoff, A.; Fayer, M. D. *Acc. Chem. Res.* **1995**, *28*, 437.
(6) Pershan, P. S. Raman studies of orientational order in liquid crystals. *The molecular physics of liquid crystals*; In Luchhurst, G. R., Gray, G. W., Eds.; Academic: London, 1979; p 385.
(7) Cates, D. A.; Mac Phail, R. A. *J. Phys. Chem.* **1991**, *95*, 2209.
(8) Ben-Amotz, D.; Lee, M. R.; Cho, S.; List, D. *J. Chem. Phys*. **1992**, *96*, 8781.
(9) Ultrashort Laser Pulses and Applications. *Topics in Applied Physics*, Vol. 60; Springer: Berlin, 1993. Kaiser, W., Ed.; Springer-Verlag: 1988.
(10) Lynden-Bell, R. M. *Mol. Phys.* **1977**, *33*, 907.
(11) Oxtoby, D. W. *J. Chem. Phys.* **1979**, *70*, 2605.
(12) Fischer, S. F.; Laubereau, A. *Chem. Phys. Lett*. **1975**, *35*, 6.
(13) Schweizer, K. S.; Chandler, D. *J. Chem. Phys*. **1982**, *76*, 2296.
(14) Dijkman, F. G.; van Maas, J. H. *Appl. Spectrosc*. **1976**, *30*, 545.
(15) Kołodziejski, M.; Waliszewska, G.; Abramczyk, H. *Chem. Phys.* **1996**, *213*, 341.
(16) Ladanyi, B. M.; Geiger, L. C.; Zerda, T. W.; Song, X.; Jonas, J. *J. Chem. Phys*. **1988**, *89*, 660.
(17) Geiger, L. C.; Ladanyi, B. M. *J. Chem. Phys.* **1988**, *89*, 6588.
(18) Ladanyi, B. M.; Stratt, R. M. *J. Phys. Chem*., in press.
(19) Bellows, J. C.; Prasad, P. N. *J. Chem. Phys.* **1979**, *70*, 1864.
(20) Hesp, B. H.; Wiesma, D. A. *Chem. Phys. Lett*. **1980**, *75*, 423.
(21) Prasad, P. N.; Kopelman, R. *J. Chem. Phys*. **1973**, *58*, 126.
(22) Chronister, E. L.; Dlott, D. D. *J. Chem. Phys.* **1983**, *79*, 5286.
(23) Hill, J. R.; Chronister, E. L.; Chang, T.-C.; Kim, H.; Postlewaite, J. C.; Dlott, D. D. *J. Chem. Phys.* **1988**, *88*, 949.
(24) Angell, C. A.; Poole, P. H.; Shao, J. *Nuovo Cimento Soc. Ital. Fis.* **1994**, *16D*, 993.
(25) Angell, C. A. *J. Phys. Chem.* **1982**, *86*, 3845.
(26) Collings, P. J.; Hird, M. *Introduction to Liquid Crystals*; The Liquid Crystals Book Series; Taylor & Francis: London, 1997.
(27) Abramczyk, H.; Kołodziejski, M.; Waliszewska, G. *Chem. Phys.* **1998**, *228*, 313.
(28) Dijkman, F. G.; van Maas, J. H. *Appl. Spectrosc*. **1976**, *30*, 545.